Numerical study of changes in coal permeability in a mining workface

***Xiang-Chao Shi*[1], *Ying-Feng Meng*[2], *Li Gao*[2], *Xu Tian*[2], *Xu Yang*[2], *Wu-Qiang Cai*[2] *and* *Shuai Mao*[2]**

At the front of a working coalface, the stress state can differ significantly across different zones. This seriously affects the permeability of the coal seam. In this study, we adopt a discrete element method to study the coal permeability under different stress states. The results indicate that an increase in stress (when $\sigma_x = \sigma_y$) causes the permeability to decrease significantly according to an exponential attenuation model. As the stress ratio (σ_x/σ_y) increases, the change in x-direction permeability is initially small. However, when the stress ratio reaches a certain value, the permeability starts to increase significantly. This is because of cracks that open under shear dilation. The change in coal permeability is examined in terms of the stress state at the front of the workface in three typical mining layouts. Our results show that the x direction permeability to the left of the peak stress increases slightly, but the y-direction permeability increases significantly. The unloading of x- and y-direction stress to the right of the peak stress causes cleats to open, resulting in a significant increase in both x and y-direction permeability.

Key words: *permeability; mining layouts; crack coal mass; discrete element method*

Introduction

Coal is a typical double-porous rock composed of matrix pores and fractures. Closely proposed a dual porous medium model consisting of cleats and matrix pores to describe the structural characteristics of coal [1]. A large number of tiny pores contained in the coal matrix form the main storage space of gas. The matrix porosity is 5.84–10.51 %, with a proportion of total porosity of some 82–90 %, but the permeability is extremely low. The cleat porosity is 0.5–2.5 %, with a proportion of total porosity of 10–18 %. The fracture width is typically 0.001–20 mm, so the cleats are the primary seepage channel for fluids (i.e., gas and water) [2]. According to the morphology and intersection relations, the cleats are named the face cleat and butt cleat.

It is generally acknowledged that fractures are the main contributor to coal's permeability, and their direction and character control the fluid flow through the coal. According to the "Cubic Law," the flow rate along a fracture is proportional to the cube of its width [3]:

$$q = \frac{gd^3}{12\mu} J \tag{1}$$

where q is the flow rate in a planar fracture, J is the hydraulic gradient, d is the width of the fracture, and μ is the dynamic viscosity coefficient of the flow.

The permeability of a fracture is affected by many factors, such as its roughness, filling degree, and, most importantly, the stress environment [4]. An increased stress loading leads to fracture closure, which decreases the permeability of the rock. Conversely, stress unloading allows the fracture to open, which increases the permeability of the rock—the same is true of coal.

One of the key factors hindering the development and extraction of coal-bed methane is low permeability in the coal seam [5]. The stress state of working faces changes as the face is worked. Figure 1 illustrates the stress state of a working face under different mining techniques [6]. We can observe three distinct stress sections: an in-situ stress zone, abutment pressure loading zone, and abutment pressure unloading zone. Fracture closing and opening change the coal permeability under the effect of loading and unloading from mining disturbances. Under such disturbances, the mechanical behavior of the coal–rock mass in front of the workface exhibits significant differences, with the abutment pressure (vertical stress) on the working face gradually increasing to a peak, then, with the destruction of the coal, advancing into the unloading state and reducing to a single-pressure residual state; the horizontal stress gradually decreases to 0 (Fig. 1). Coal with a large number of fractures will change tremendously with these variations in stress state. This paper studies the influence of mining on the permeability of coal using a discrete element method.

[1] *Xiang-Chao Shi*, State Key Laboratory of Oil and Gas Reservoir Geology and Exploitation, Southwest Petroleum University, Chengdu 610500, China, State Key Laboratory of Hydraulics and Mountain River Engineering, College of Water Resources and Hydropower, Sichuan University, Chengdu 610065, China, sxcdream@163.com

[2] *Ying-Feng Meng, Li Gao, Xu Tian, Xu Yang, Wu-Qiang Cai , Shuai Mao,* State Key Laboratory of Oil and Gas Reservoir Geology and Exploitation, Southwest Petroleum University, Chengdu 610500, China

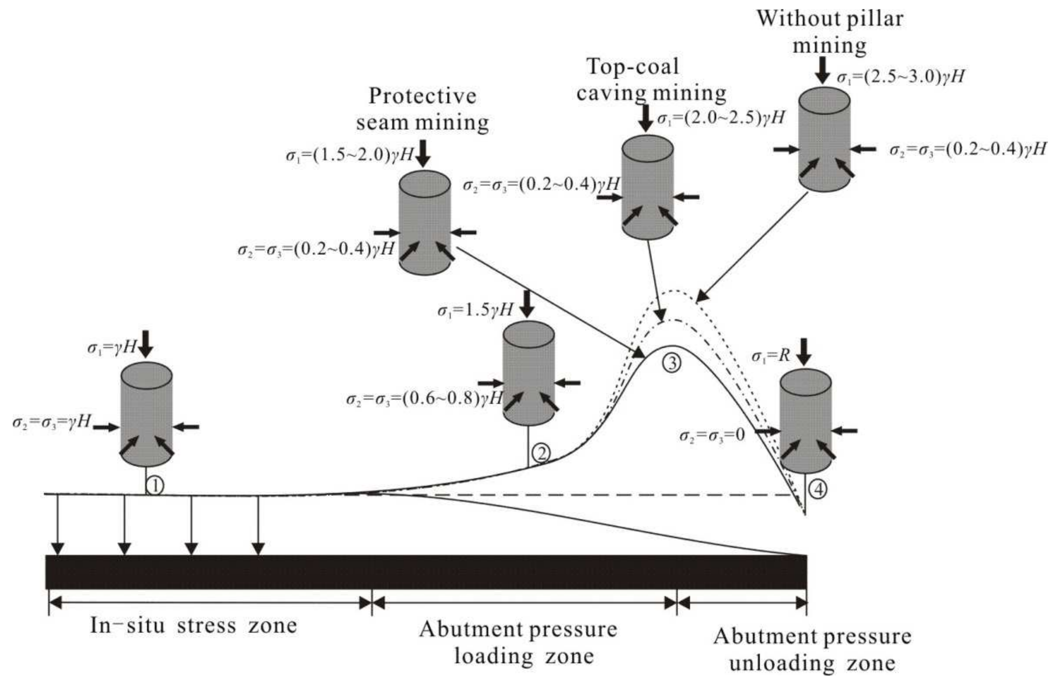

Fig. 1. Stress state of coal at the front of a workface for different mining layouts (γ is the volume weight; H is the depth; σ_1 is the maximum main stress; σ_2 the intermediate principal stress; σ_3 is the minimum principal stress).

Numerical Simulation of Coal Permeability in Different Mining Layouts

2.1 Mathematical model of hydromechanical coupling in a fracture

When the cleats close under loading stress, the supporting objects will support the cleat surface. Under an unloading stress, the cleats open via matrix elastic rebound, as shown in Figure 2. The initial fracture width is d_0, and the change in fracture width under normal stress is Δd. Thus, the width of the fracture under normal stress d is

$$d = d_0 + \Delta d \tag{2}$$

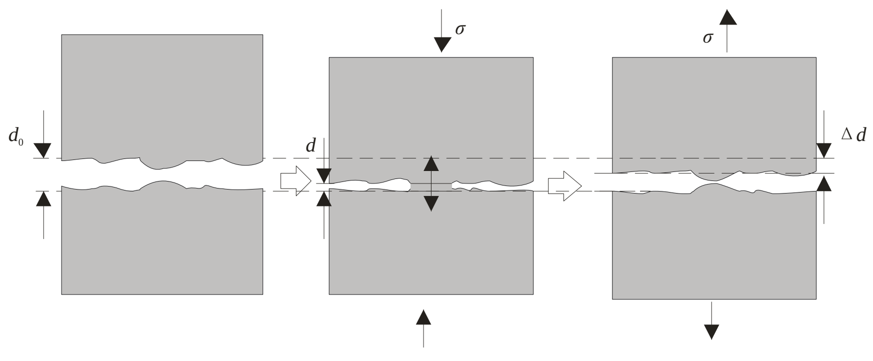

Fig. 2. Model for the change of fracture width under stress loading.

The discrete element method assumes there is a linear relationship between stress and displacement on the joint surface. This relationship is controlled by the rigidity coefficient of the joint surface k_n, so the effective stress increment is

$$\Delta\sigma_n = -k_n \Delta d \tag{3}$$

where Δd is the normal displacement increment.

The constitutive relation of the joint surface obeys the Mohr–Coulomb criterion of shear strength:

$$|\tau| \le C + \sigma \tan\phi = \tau_{\max} \tag{4}$$

where C is the cohesion force and ϕ is the internal friction angle.

The relationship between shear stress and shear displacement increment is controlled by the shear stiffness k_s :

$$\Delta\tau_s = -k_s \Delta u_s^e \tag{5}$$

where Δu_s^e is the shear displacement increment, $\Delta\tau_s$ is the shear stress increment, and $|\tau_s| \leq \tau_{\max}$.

When $|\tau_s| \geq \tau_{\max}$,

$$\tau_s = sign(\Delta u_s)\tau_{\max} \tag{6}$$

where Δu_s is the total shear displacement increment.

The Mohr–Coulomb model is adopted to reflect the dilatancy effect of the joint:

$$\left.\begin{array}{ll} when|u_s| < u_{cs} & u_s = u_n^d \tan\psi \\ when|u_s| \geq u_{cs} and |\tau_s| = \tau_{\max}, \text{ or } |\tau_s| \leq \tau_{\max} & \psi = 0 \end{array}\right\} \tag{7}$$

where u_s is the joint shear displacement, u_{cs} is the limit shear displacement of dilatancy, and u_n^d is the normal displacement component.

As fluid flow in a fracture obeys the cubic law, the flow rate can be given by

$$q = -\lambda_j d^3 \frac{\Delta p}{L} \tag{9}$$

where λ_j is the permeability factor (which has a theoretical value of $1/12\mu$, where μ is the dynamic viscosity coefficient of the flow).

The change in pore pressure through the contacts is as follows:

$$\Delta p = \frac{K_w}{V}\left(\sum Q\Delta t - \Delta V\right) \tag{10}$$

where $\sum Q$ is the sum of the flow rates from all surrounding contacts, ΔV is the pore volume change in the domain areas, V is the new pore volume, K_w is the bulk modulus of the fluid, and Δt is the time step.

2.2 Coal fracture network model

The Monte-Carlo method is widely used to simulate random joints in rock [7, 8]. Based on Monte-Carlo method, we wrote a program in the FISH language (embedded in UDEC) to generate a random fracture network. The geometrical cleat parameter for coal is shown in Table 1, and the simulation results are shown in Figure 3.

Tab. 1. Random cleat parameters.

Joint set	Dip angle [°] (normal distribution)		Mean trace length [m] (normal distribution)		Joint sparing [m]
	Average value	Standard deviation	Average value	Standard deviation	Average value
Face cleat	0	5	0.6	0.2	0.2
Butt cleat	90	5	0.2	0.04	0.4

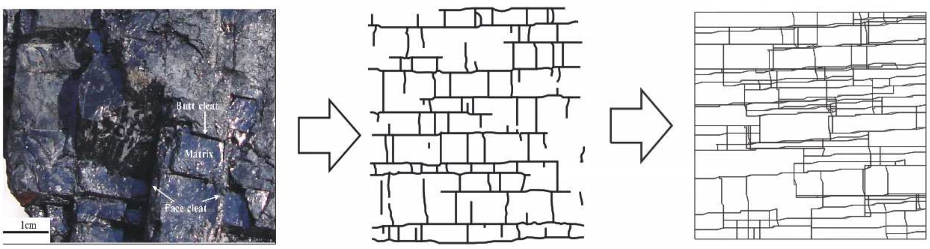

Fig. 3. Fracture network model of coal.

The equivalent permeability of coal can be calculated by [9]

$$\left.\begin{aligned} K_x &= \frac{q_x l_x}{l_y \Delta P_p} \\ K_y &= \frac{q_y l_y}{l_x \Delta P_p} \end{aligned}\right\} \tag{8}$$

where l_x and l_y is respectively the section length of fluid flow though *x*, *y* direction, ΔP_p is the pressure difference from two section, Q_x and Q_y is respectively fluid low though x, y direction.

2.3 Parameters and boundary conditions

The stress sensitivity of coal cleat permeability is simulated using random cleats. The mechanical parameters adopted in the simulation are listed in Table 2, and the boundary conditions are shown in Figure 4. The mechanical boundary conditions are imposed in the x- and y-directions (Fig. 4(a)). When studying the permeability in the x-direction, the pore pressure of the left side is P_p = 6 MPa and that of the right side is P_p = 0 MPa. The upper and lower edges of the model are set to be impermeable boundaries (Fig. 4(b)). When studying the permeability in the y-direction, the left and right sides are set to be impermeable boundaries, with the pressure at the upper boundary set to P_p = 6 MPa and that at the lower boundary set to P_p = 0 MPa (Fig. 4(c)).

Tab. 2. Mechanical parameters of model.

Mechanical properties of coal rock	Elasticity modulus [MPa]	2900
	Poisson's ratio	0.38
Mechanical properties of joint	Normal stiffness [MPa]	2700
	Shear stiffness [MPa]	2550
	Cohesion [MPa]	5
	Internal friction angle [°]	35
	Dilatation angle [°]	5
	Initial width [mm]	0.005
	Residual width [mm]	0.002

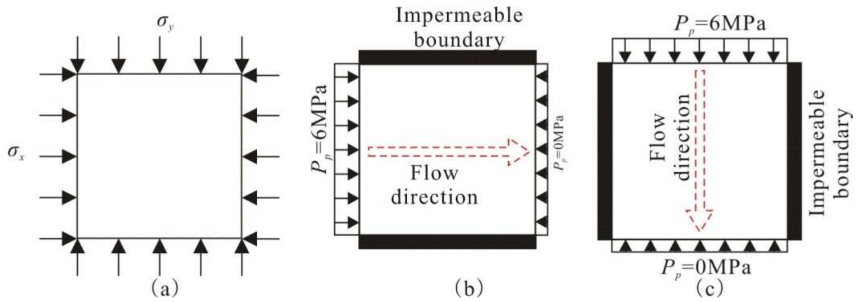

Fig. 4. Boundary conditions of model.

For the stress boundary conditions, we adopt three schemes:

1. Set the stress in the x- and y-directions to have the same increments. The mechanical boundary conditions are listed in Table 3.

Tab. 3. Mechanical boundary conditions for the same stress ratio.

σ_x [MPa]	σ_y [MPa]	σ_x / σ_y
2	2	1
4	4	1
8	8	1
10	10	1

2. Set the stress in the y-direction to $\sigma_y = 5\text{MPa}$, and change the x-direction stress σ_x to study the permeability change under different stress ratios σ_x / σ_y. The mechanical boundary conditions are then as given in Table 4.

Tab. 4. Mechanical boundary conditions for different stress ratios.

σ_x [MPa]	σ_y [MPa]	σ_x / σ_y

5	5	1
8	5	1.6
10	5	2
12	5	2.4
15	5	3
18	5	3.6
20	5	4
25	5	5

3. Set the mechanical boundary conditions according to the stress state of the working face in three typical mining layouts. The mechanical boundary conditions at different positions along the front of the workface illustrated in Figure 1 are listed in Table 5.

Tab. 5. Mechanical boundary conditions for different mining layouts.

Mining layouts	**Stress position**	σ_x [MPa]	σ_y [MPa]
Mining without pillars	①	10	10
	②	7	15
	③	3	27.5
	④	0	2
Top-coal caving mining	①	10	10
	②	7	15
	③	3	22.5
	④	0	2
Protective layer mining	①	10	10
	②	7	15
	③	3	17.5
	④	0	2

Simulation Results

3.1 Permeability of coal under different stress conditions

The change in coal permeability with respect to stress in the *x*- and *y*-directions is shown in Figure 5. This shows that the relation between stress and permeability agrees with an exponential attenuation model for $\sigma_x = \sigma_y$.

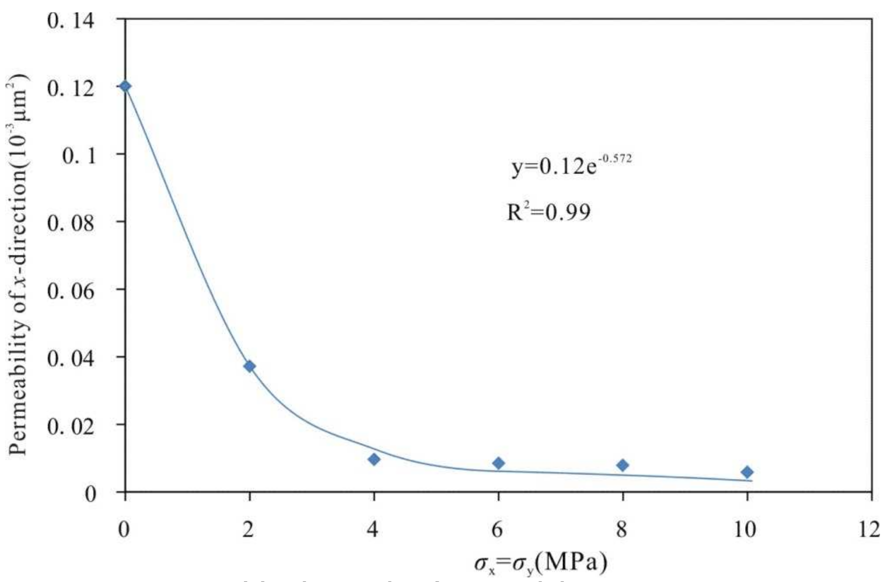

Fig. 5. Permeability change in the x-direction with the same stress increment.

The coal permeability under different stress ratios is presented in Figure 6. The permeability in the *x*-direction decreases slightly when $\sigma_x / \sigma_y < 2.4$. This is due to the closing of *x*-directional cleats under the stress loading condition. However, when $\sigma_x / \sigma_y > 2.4$, the permeability increases significantly with the stress ratio, as there is more volume compression in the *x*-direction and volume expansion in the *y*-direction.

When the stress is sufficient to overcome the joint strength, shear expansion of the fracture occurs, and the fracture width becomes larger. This increases the flow capacity of the fracture, characterized by an increase in permeability.

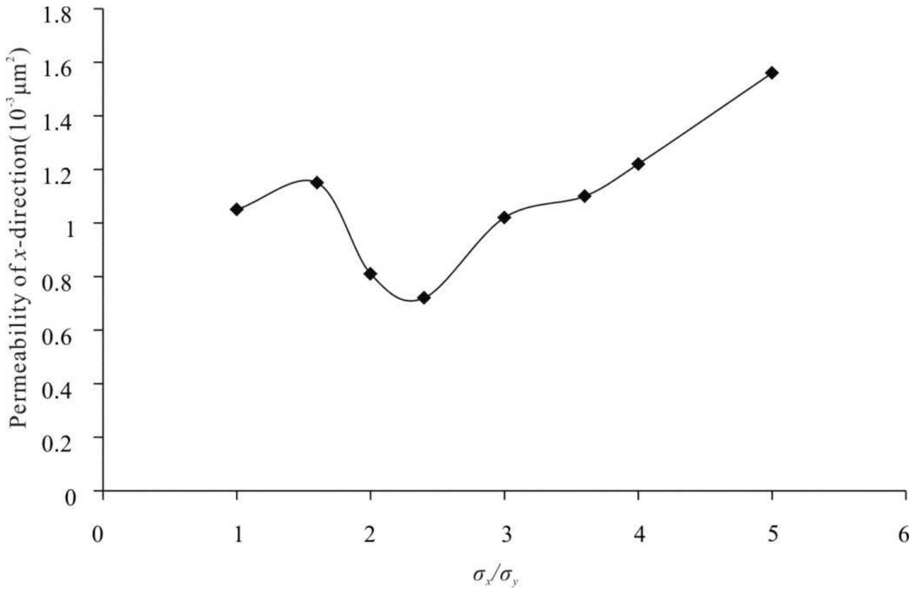

Fig. 6. Permeability in the x-direction with respect to σ_x / σ_y .

3.2 Permeability changes in a coal workface for different mining layouts

Simulation results for the permeability of coal under different mining conditions are shown in Figures 7 and 8. It can be observed from Figure 7 that the permeability in the *x*-direction changes slightly to the left of point ③ . This is because the unloading of stress in the *x*-direction has a slight effect on the *x*-direction permeability. The permeability to the right of point ④ increases significantly, as the stress close to the workface at point ④ is extremely low, causing the cleats to open.

Figure 8 indicates that the permeability in the *y*-direction increases significantly in the loading zone to the left of stress peak point ③. This is because the stress loading in the *y*-direction and unloading in the *x*-direction cause the *y*-directional cleats to open and the *y*-direction tensile fracture to increase. The permeability in the unloading area to the right of stress peak point ③ increases rapidly, for the same reasons as in Figure 7. The permeability is affected slightly by different mining layouts for different stress conditions.

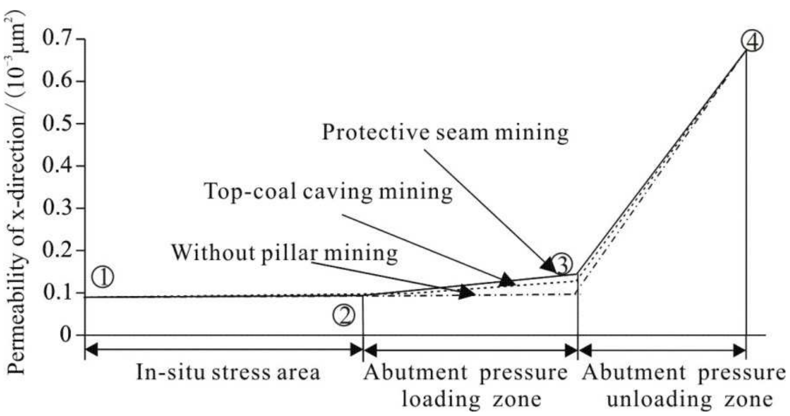

Fig. 7. Permeability in the x-direction under different mining layouts (Points ①, ②, ③, ④ are consistent with those in Figure 1).

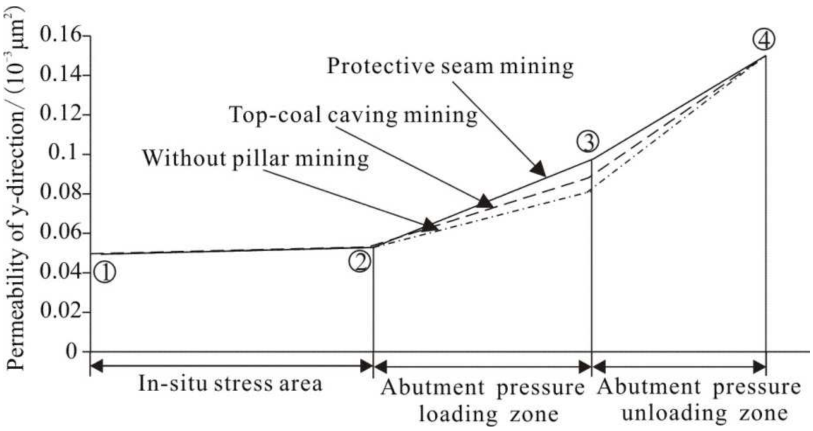

Fig. 8. Permeability in the y-direction under different mining layouts (Points ①, ②, ③, ④ are consistent with those in Figure 1).

Conclusions

In this paper, we have examined the change in permeability of a coal workface under various stress conditions. Our main contributions have been:

1. Using Monte-Carlo theory, we wrote a FISH program to generate random fracture networks. The program can effectively simulate the cleats found in coal seams.
2. The stress condition was shown to be the main factor in the permeability of coal cleats. The closure of these cleats with increases in stress causes a decrease in permeability that follows an exponential attenuation model.
3. When the stress ratio σ_x/σ_y reaches a certain value, the permeability increases significantly. This occurs when the stress reaches the joint strength, at which point the fractures open, enhancing the connectivity and increasing permeability.
4. Different stress conditions can be found in different mining layouts, meaning that the permeability of different stress zones across a workface will vary. The *x*-direction permeability to the left of the peak stress point was found to increase slightly, but the *y*-direction permeability increased significantly with the change in stress state. The *x*- and *y*-direction permeability close to the workface increased rapidly when the cleats were opened by stress unloading in the *x*- and *y*-directions.

Acknowledgements: *This work was financially supported by national natural science funds of China (Number: 51504208), the Open Fund (Number: PLN1421) of the State Key Laboratory of Oil and Gas Reservoir Geology and Exploitation (Southwest Petroleum University), the SWPU Science & Technology Fund (Number: 2013XJZ029) and the scientific fund of the Sichuan provincial education department (Number: 14ZB0060)*

References

[1] Close J. C.: Natural fractures in coal, Hydrocarbons from coal: *AAPG Studies in Geology, vol. 38, pp. 119-132, 1993.*

[2] Laubach S. E., Marrett R. A., Olson J. E., Scott A. R.: Characteristics and origins of coal cleat: A review, *International Journal of Coal Geology, vol. 35, no. 1, pp. 175-207, 1998*.

[3] Snow D. T.: A parallel plate model of fractured permeable media, *California, USA: University of California, 1965*.

[4] Somerton W. H., Söylemezoǧlu I. M.,Dudley R. C.: Effect of stress on permeability of coal, *International Journal of Rock Mechanics and Mining Sciences & Geomechanics Abstracts, vol. 12, no.5–6: pp. 129-145, 1975.*

[5] Cheng Y., Wang H., Wang L., Ma X.: Principle and engineering application of pressure relief gas drainage in low permeability outburst coal seam, *Mining Science and Technology (China), vol 19, no.3, pp. 342-345, 2009.*

[6] Xie H., Zhou H., Liu J., Gao F., Zhang R., Xue D., Zhang Y.: Mining-induced mechanical behavior in coal seams under different mining layouts, *Journal of China Coal Society(China), vol. 36, no. 7, pp.1067-1075, 2011*.

[7] Maiti S., Tiwari R. K.: A hybrid Monte Carlo method based artificial neural networks approach for rock boundaries identification: A case study from the KTB bore hole, *Pure and Applied Geophysic, vol. 166. No.12, pp. 2059-2090, 2009.*

[8] Bosch M., Meza R., Jiménez R., Hönig A.: Joint gravity and magnetic inversion in 3D using Monte Carlo methods, *Geophysics, vol.71, no. 4, pp.153-156, 2006*.

[9] Zhang X., Sanderson D. J.,. Harkness R. M, Last N. C.: Evaluation of the 2-D permeability tensor for fractured rock masses, *International Journal of Rock Mechanics and Mining Sciences & Geomechanics Abstracts, vol.33, no. 1, pp. 17-37, 1996.*